Implications of Rarefied Gas Damping for RF MEMS Reliability

Alina Alexeenko and Sruti Chigullapalli

Department of Aeronautics and Astronautics, Purdue University

Abstract.
Capacitive and ohmic RF MEMS switches are based on micron-sized structures moving under electrostatic force in a gaseous environment. Recent experimental measurements [4, 5] point to a critical role of gas-phase effects on the lifetime of RF MEMS switches. In this paper, we analyze rarefied flow effects on the gas-damping behavior of typical capacitive switches. Several damping models based on Reynolds equation [7, 8] and on Boltzmann kinetic equation [9, 6] are applied to quantify the effects of uncertainties in fabrication and operating conditions on the impact velocity of switch contact surfaces for various switch configurations. Implications of rarefied flow effects in the gas damping for design and analysis of RF MEMS devices are discussed. It has been demonstrated that although all damping models considered predict a similar damping quality factor and agree well for predictions of closing time, the models differ by a factor of two and more in predicting the impact velocity and acceleration at contact. Implications of parameter uncertainties on the key reliability-related parameters such as the pull-in voltage, closing time and impact velocity are also discussed.

Keywords: MEMS, gas damping,uncertainty quantification
PACS: 07.10.Cm,47.61.-k,47.45.-n

INTRODUCTION

One class of MEMS that is projected to have an amazing growth in the next decade is the radio-frequency (RF) MEMS switches [1]. However, uncertainties in the reliability of RF MEMS switches and tunable capacitors are still a major hurdle on the road to widespread commercial adaptation of the RF-MEMS technology. Improved knowledge of aging mechanisms and the fundamental physics of failure of capacitive RF-MEMS is necessary for development of reliable design practices for such systems. Common failure mechanisms in MEMS include both mechanical (viscoelasticity, creep) and electrical (dielectric leakage, charging, and breakdown) degradation. In capacitive MEMS the most commonly observed failure mode is stiction of the metal membrane to the solid dielectric surface during contact. It has been observed that the dynamics of switch closing when the contact occurs has a significant impact on the performance and lifetime. Additionally, the lifetime of capacitive MEMS switches strongly depends on gas pressure [4]. Czarnecki et al.[3] have demonstrated that under the same actuation, the switch tested at atmospheric pressure had a lifetime of more than a million cycles whereas at 200$mbar$ and 20$mbar$ the switches failed after $330,000$ and 200 cycles, respectively. To accurately predict the impact velocity and other dynamical parameters of such switches, we develop high-fidelity simulations of gas damping under various conditions and apply them to study the stochastic dynamics of a single closing event of a typical capacitive switch.

The choice of a physical model to describe adequately a gas flow depends on the flow regime. A map of flow regimes in terms of Knudsen and Mach numbers and applicable governing equations are shown in Figure 1a. The low-speed flows can often be described by the Reynolds equation, a simplified form of the Navier-Stokes equations with negligible convective terms. The Reynolds equation is often used to describe fluidic effects in microsystems with gas confined in long gaps. However, the Reynolds and Navier-Stokes description breaks down when the characteristic size decreases and the flow transitions to rarefied regime. The Boltzmann equation is a general form of the gas transport equation based on the kinetic theory and can be reduced to Navier-Stokes equations in the near-continuum limit. The challenge of selecting an adequate description for gas damping in MEMS switches consists in the fact that the Knudsen number varies during the switch operation. At one-atmosphere air, the Knudsen number is typically in continuum ($Kn < 0.01$) and slip flow ($0.01 < Kn < 0.1$) regimes for a typical switch in "Up-state" position corresponding to the maximum static gap. As the gap between beam and the pull-down electrode closes to "Down-state", the Knudsen number increases and results in free-molecular flow. Figure 1b shows the normalized pressure contours and and streamlines for $Kn = 4.0$ and $Kn = 0.04$ from Boltzmann-ESBGK solution. The Boltzmann equation, although

significantly more involved, offers a modeling framework that is applicable for the entire range of Knudsen numbers encountered during a switch actuation.

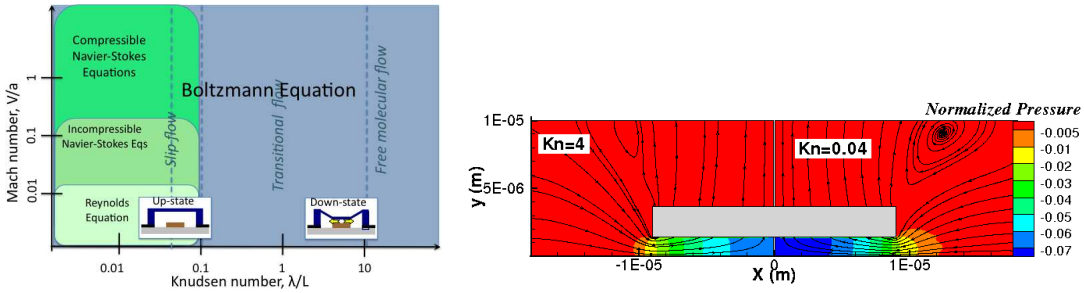

FIGURE 1. (a) Map of flow regimes. (b) Pressure contours and streamlines for $Kn = 4.0, 0.04$

APPLICATION: ANALYSIS OF DYNAMICS OF A MEMS SWITCH

In this section we apply the gas damping models for analysis of dynamics of a MEMS switch with experimentally measured uncertainties in geometry and mechanical properties.

Device Fabrication and Uncertainty Measurements

The device structure is representative of a standard RF MEMS capacitive switch. The entire device is fabricated onto an oxidized Silicon substrate. There are three electrodes of varying width underneath an electroplated Nickel fixed-fixed beam (fixed on both ends). A diagram of the switch can be seen in Figure 2. The mean, standard deviation, coefficient of variation, skewness, and kurtosis for the experimental data are given in Table 1.

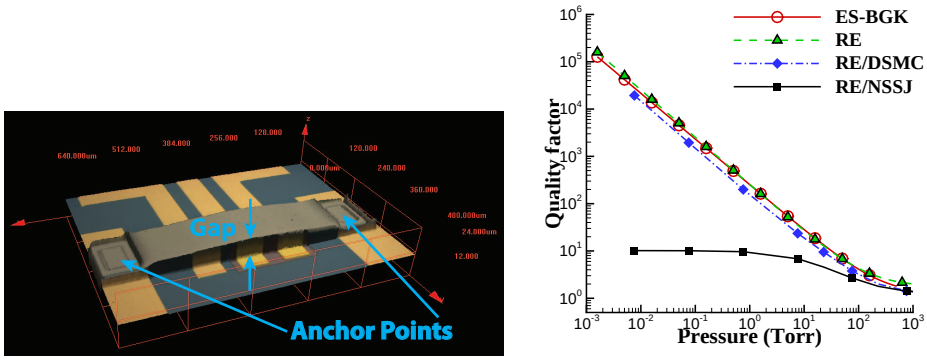

FIGURE 2. (a) Schematic of the capacitive switch test structure (Courtesy: Purdue PRISM Center/Peroulis group) (b) Comparison of quality factors for Mode 1

Switch Dynamics Model

The equation of motion of the beam in one-dimension is [2]:

$$M\ddot{X}(t) + c_f\dot{X}(t) + KX(t) = \frac{V^2}{2}\left[\frac{\varepsilon_0 A}{(g - X + t_d/\varepsilon_r)^2}(1+\alpha)\right] \tag{1}$$

TABLE 1. Experimentally measured device uncertainties

data	Mean (μ)	std (σ)	COV, %	skewness	kurtosis
Length, L (μm)	509.54	0.70	0.14	-0.35	2.25
Width, w (μm)	122.93	0.56	0.46	0.56	3.31
Gap-size, g (μm)	3.49	0.22	6.3	0.20	1.75
Thickness, t (μm)	4.0	0.35	8.75	1.14	3.8
Effective Young's Modulus, $E(GPa)$	295.78	28.93	9.78	-0.10	1.74
Fringing Field coefficient, α	1.34	0.1513	-	-	-
Damping coefficient, A	10.39	1.04	-	-	-

TABLE 2. Correlated variables

data	mean	std	COV, %	skewness	kurtosis
Effective mass, $M(\mu g)$	1.10	0.10	8.95	0.04	3.0
Effective stiffness, $K(N/m)$	368.52	103.60	28.11	0.61	3.54
Pull-in Voltage, $V_{pi}(V)$	123.38	21.16	17.15	0.35	3.11

with initial conditions $X(0) = 0, \dot{X}(0) = 0$ where X is the displacement of the beam, c_f is the damping factor, V is the actuation voltage, g is the gap-size, t_d is the thickness of dielectric layer with relative permittivity $\varepsilon_r = 8.5$, ε_0 is the permittivity of air and $A = 3b_0w$ is the total overlap area between the beam and three electrodes. M, K, L, w and t denote the effective mass, stiffness, length, width and thickness of the beam respectively. This reduced order model provides a good representation of the dynamics of switch to uncertainties in the input quantities and the gas damping models. The effective stiffness of a fixed-fixed beam with the force evenly distributed about the center of the beam is

$$K = \frac{32Ew}{8(\frac{x}{L})^3 - 20(\frac{x}{L})^2 + 14(\frac{x}{L}) - 1}(\frac{t}{L})^3 \tag{2}$$

where $x = (L+b)/2)$ and b is the effective width of electrode calculated as $b = 3 * b_0 * w$. Given the effective stiffness, the resonant frequency of the device can be calculated using $\omega_n = \sqrt{\frac{K}{M}} = \beta^2\sqrt{\frac{EI}{\rho wtL^4}}$ where ρ is the density of the material, I is the moment of inertia given by $wt^3/12$, and for the first mode of a fixed-fixed beam β is 4.73004. Therefore, the effective mass is

$$M = \frac{12K\rho L^4}{\beta^4 Et^2} \tag{3}$$

By equating the applied electrostatic force with the mechanical restoring force due to the stiffness of the beam, we have $F_e = KX$. Solving the equation for the voltage and setting $X = \frac{g_0 + t_d/\varepsilon_r}{3}$ at point of instability, the pull-in voltage for the switch can be found by Eq (4). The mean, standard deviation, coefficient of variation, skewness, and kurtosis for the correlated variables are given in Table 2.

$$\mathrm{V_{pi}} = \sqrt{\frac{8\mathrm{K}}{27\varepsilon_0 A(1+\alpha)}}(g_0 + \mathrm{t_d}/\varepsilon_\mathrm{r})^{1.5} \tag{4}$$

Sensitivity Analysis

Using a first order Smolyak sparse grid [10], the response surface for impact velocity and closing time were calculated based on 11 samples generated from 5 input variables t, g, E, α, A. The response surfaces of impact velocity and closing time had a fit of $R^2 = 1$ and 0.98 respectively and their equations are:

$$V_{rs} = 185.86 - 0.686 * t + 0.728 * g + -0.011688 * E + 53.085 * \alpha - 12.387 * A \tag{5}$$

$$t_{rs} = -189.144 + 20.343 * t + 29.572 * g + 0.089 * E - 14.93721 * \alpha + 1.915 * A \tag{6}$$

TABLE 3. Coefficients of variables in response surface.

Variable	Impact VelocityV/V_o	Closing time t_{close}/t_{close0}
$\tilde{t}$	-0.022	3.806
$\tilde{g}$	0.020	4.827
$\tilde{E}$	-0.0277	1.218
$\tilde{\alpha}$	0.5709	-0.937
$\tilde{A}$	-1.024	0.9234

Converting this to a function of non-dimensional parameters $\tilde{t} = t/t_0 - 1$ and so on, the coefficients are shown in Table 3. The negative sign of the coefficient for A, E and t in Eq(5) suggests that the impact velocity decreases as the thickness, Young's Modulus and damping coefficient increase. The higher the magnitude of a coefficient, the greater is the sensitivity of output variable with respect to that input parameter. Therefore, from the coefficients it can be seen that the impact velocity is most sensitive to the damping model coefficient and least sensitive to gap and the closing time is most sensitive to geometric parameters g and t.

Results and Discussion

Effect of Gas Damping Model: The effect of using different gas damping models in the switch dynamics simulations has been studied first. Here we compare three models: (i) a model based on unsteady Reynolds equation [7]; (ii) a model based on a modified Reynolds equation with the first-order slip boundary conditions formulated from DSMC simulations [8] (iii) compact model based on Boltzmann-ESBGK simulations [9]. As shown in Fig. 2b, overall good qualitative agreement has been observed for quality factors ($Q = \frac{\rho wt\omega}{C_f}$) predicted by the three models.

The three models are then used for prediction of dynamics of a single switching event for the switch with mean properties (as listed in Table 1. All simulations are stopped when the switch gap reaches the surface roughness of $50nm$. The predictions of displacement, velocity, acceleration of the Nickel fixed-fixed beam using three models for an ambient pressure of $P = 1atm$ are shown in Figures 3. For the actuation voltage $V_{90} = 147.5V$, we can in general observe that the profile for the switch gap from Reynold's equation and Gallis-Torczynski match well up to $g = 2.2\mu m$ and then tend to deviate. Towards the end, the velocity profiles from compact model and Reynold's model have the same shape (increasing trend with time) whereas the one from Gallis-Torczynski model is significantly different. The difference between the predictions of these three models is attributed to the different parameter ranges for which the models have been generated. In particular, the Reynolds-equation model has a limited validity in terms of the range of Knudsen numbers. The ESBGK model has been generated for a wide range of Knudsen numbers ($0.05<Kn<50$). Additionally, all of the models were generated with the assumption of the beam thickness being less than or equal to the gap size. This assumption is not valid at the near-contact region.

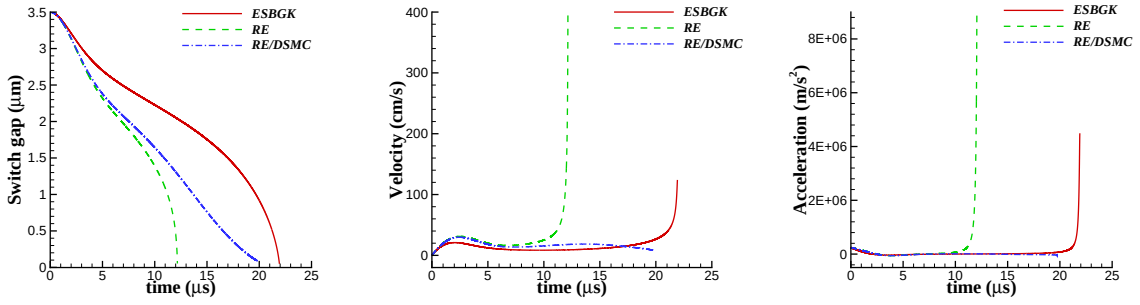

FIGURE 3. Effect of various gas damping models: a)compact model (ESBGK) and b)Veijola's model (RE) c) Gallis-Torczynski model (RE/DSMC) on the impact velocity and closing time of a Ni switch actuated at $147.5V$.

Effect of ambient gas pressure: Figure 4 show the simulated variation of switch gap, velocity and acceleration of the Ni beam versus time at three different pressures (0.01 atm, 0.1atm and 1atm) when the actuation voltage of $V_{90} = 147.5V$ is applied to the switch at hand. The compact model for damping is used here. As seen in Figure 4a, higher pressures result in higher switching times. For example an approximate $4\times$ increase in switching time is observed when the

pressure is increased by $100\times$ (from $0.01atm$ to $1atm$). The pressure effect is even more pronounced on the switch impact velocity and acceleration at contact as shown in Figure 4b,c. The impact velocity is increased by almost $6\times$ when the pressure is decreased by $100\times$.

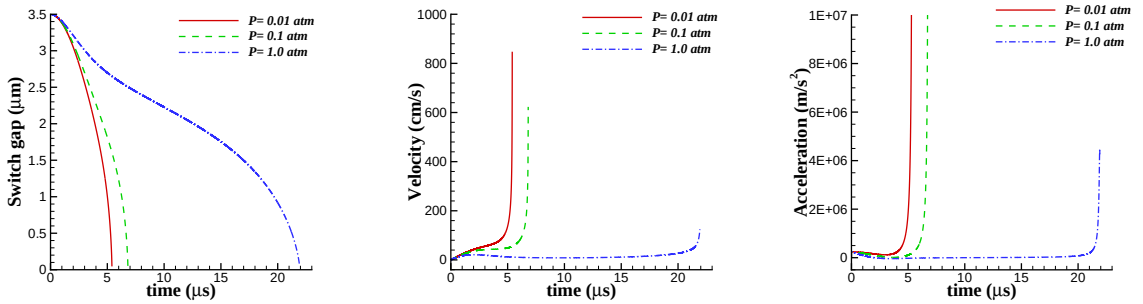

FIGURE 4. Effect of ambient gas pressure on the impact velocity and closing time of a Nickel fixed-fixed beam actuated at 90% pull-in bias of 147.5 V

Effect of device-to-device variability: Finally, we consider how the uncertainty in geometric parameters and mechanical properties affects the dynamics of such switches. Table 4 shows the mean, standard deviation, coefficient of variation, skewness, and kurtosis for the output pdfs of closing time and impact velocity from simulations on a device sample size of 1000. Gaussian input pdfs of thickness, switch gap and effective Young's Modulus were chosen with the mean and standard deviation from table 1. Uniform input pdfs were chosen for the fringing field and damping coefficients α and A respectively. The coefficient of variation is as high as 40.0% for closing time at $V_{90} = 147.5V$ for given input coefficients of variation of $6.3\%, 8.75\%$ and 9.86% for thickness, switch gap and Young's modulus respectively.

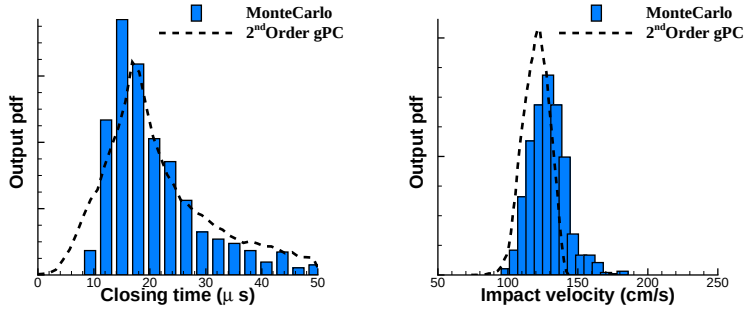

FIGURE 5. Output pdf of closing time and impact velocity of a sample (N=1,000) of switches activated at 147.5 V using Monte Carlo and a 2^{nd} order response surface.

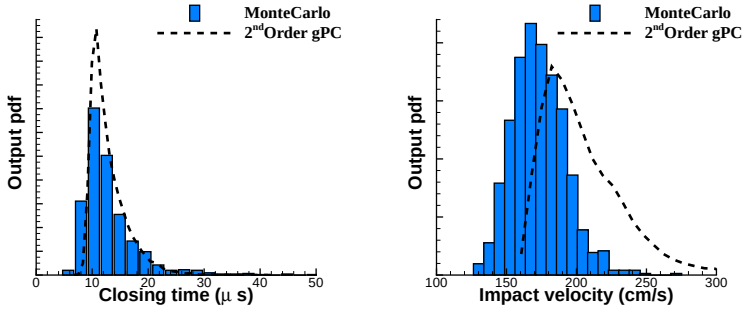

FIGURE 6. Output pdf of closing time and impact velocity of a sample (N=1,000) of switches activated at $172.5V$ using Monte Carlo and a 2^{nd} order response surface

TABLE 4. Uncertainty in output pdf of closing time and impact velocity for given uncertainty in t, g, E, α and A

Quantity	mean	std	COV, %	skewness	kurtosis
Actuation at 90% pull-in voltage (147.5 V)					
Closing time (μs)	20.73	8.268	39.88	1.323	4.41
Impact velocity (cm/s)	128.95	12.66	9.82	0.67	4.21
Actuation at 99% pull-in voltage (172.5 V)					
Closing time (μs)	13.0	5.05	38.90	2.51	12.55
Impact velocity (cm/s)	173.01	19.17	11.06	0.61	4.17

CONCLUSIONS

In this paper we have demonstrated the influence of gas damping and device-to-device variability on the closing time and impact velocity of capacitive RF MEMS switches. A number of different gas damping models spanning the range of continuum to rarefied gas flow are studied and their predictions are discussed. It is found that although both continuum models - based on the Reynolds equation - and the rarefied models - based on Boltzmann equation - give similar predictions for the closing time, the impact velocity varies by more than a factor of two. Since gas damping in typical RF MEMS switches near contact occurs in the free-molecular regime which is formally not described by continuum flow theories, the rarefied flow model is employed to calculate the impact switch velocity under uncertain condition. Specifically we consider a switch fabricated and characterized at Purdue university using a typical fabrication process. The uncertainty in the gap (6.3%) and thickness (8.8%) of the structure dominate the uncertainty of its actuation voltage (17%). Response surfaces of impact velocity and closing time to 5 input variables were constructed using first order Smolyak sparse grid algorithm. This sensitivity analysis showed that impact velocity is most sensitive to the damping model coefficient and the closing time is most sensitive to geometric parameters gap and thickness of beam. A conservative approach of applying the 90% actuation voltage is studied first. This case yields an average impact velocity of 129 cm/sec. A more realistic approach of actuating the average switch with a voltage that would result in successful actuation of 99% of the fabricated switches is considered next. This time the average impact velocity is increased to 173 cm/sec. Since a higher impact velocity results in higher damage at the contact interface, these results underline the importance of carefully considering the process-induced switch variations in the design process.

ACKNOWLEDGMENTS

The authors are grateful for support from the Purdue PRISM center under Department of Energy (National Nuclear Security Administration) award number DE-FC52-08NA28617.

REFERENCES

1. SEMI/Yole Development,*Global MEMS/Micro-systems Markets and Opportunities,*(2008).
2. G. M. Rebeiz, *RF MEMS.* Wiley, 2003.
3. P. Czarnecki, X. Rottenberg, R. Puers, I. De Wolf, Impact of Biasing Scheme and Environment Conditions on the Lifetime of RF-MEMS Capacitive Switches,*Proceeding of MEMSWAVE,* pp.133-136,(2005)
4. P. Czarnecki, X. Rottenberg, R. Puers, and I. de Wolf, Effect of Gas Pressure on the Lifetime of Capacitive RF MEMS Switches, *19th IEEE International Conference on MEMS,* pp. 890–893 (2006).
5. J. Muldavin, C. Bozler, S. Rabe, P. Wyatt, and C. Keast, *Proceedings of GOMAC,*(2009).
6. R. Bidkar, R. Tung, A. Alexeenko, H. Sumali, A. Raman, *Applied Physics Letters,* **94**, 163117, (2009).
7. T. Veijola, *J. Micromech. Microeng.* **14**, pp:1109–1118 (2004)
8. M. A. Gallis and J. R. Torczynski,*J. Microelectromech. Syst.,* **13** pp. 653–659.
9. X. Guo and A. Alexeenko,*J. of Micromech. Microeng.,* **19**, 045026, (2009)
10. S. Smolyak, *Soviet Math.* Dokl. 4, 1963, pp:240–243.